JOURNAL OF NATURAL PRODUCTS

Article

pubs.acs.org/jnp

# Alkaloids from *Hippeastrum argentinum* and Their Cholinesterase-Inhibitory Activities: An in Vitro and in Silico Study

Javier E. Ortiz,[†] Natalia B. Pigni,[‡,§] Sebastián A. Andujar,[⊥] German Roitman,[∥] Fernando D. Suvire,[⊥] Ricardo D. Enriz,[⊥] Alejandro Tapia,[†] Jaume Bastida,[‡] and Gabriela E. Feresin*[,†]

[†]Instituto de Biotecnología, Facultad de Ingeniería, Universidad Nacional de San Juan, Avenida Libertador General San Martín 1109 (O), 5400 San Juan, Argentina

[‡]Departament de Productes Naturals, Biologia Vegetal i Edafologia, Facultat de Farmàcia, Universitat de Barcelona, Avenida Joan XXIII s/n, 08028 Barcelona, Spain

[§]ICYTAC-CONICET, Departamento de Química Orgánica, Facultad de Ciencias Químicas, Universidad Nacional de Córdoba, 5000 Córdoba, Argentina

[⊥]Facultad de Química, Bioquímica y Farmacia, Universidad Nacional de San Luis, Chacabuco 915, 5700 San Luis, Argentina

[∥]Cátedra de Jardinería, Facultad de Agronomía, Universidad de Buenos Aires, Avenida San Martín 4453, 1417 Buenos Aires, Argentina

Supporting Information

**ABSTRACT:** Two new alkaloids, 4-*O*-methylnangustine (**1**) and 7-hydroxyclivonine (**2**) (montanine and homolycorine types, respectively), and four known alkaloids were isolated from the bulbs of *Hippeastrum argentinum*, and their cholinesterase-inhibitory activities were evaluated. These compounds were identified using GC-MS, and their structures were defined by physical data analysis. Compound **2** showed weak butyrylcholinesterase (BuChE)-inhibitory activity, with a half-maximal inhibitory concentration ($IC_{50}$) value of 67.3 ± 0.09 μM. To better understand the experimental results, a molecular modeling study was also performed. The combination of a docking study, molecular dynamics simulations, and quantum theory of atoms in molecules calculations provides new insight into the molecular interactions of compound **2** with BuChE, which were compared to those of galantamine.

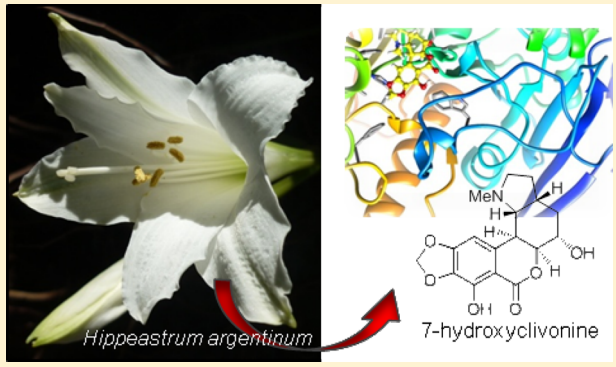


The genus *Hippeastrum*, which belongs to the Amaryllidaceae family, is endemic to South America and is characterized by large bulbs and prominent and colorful flowers. In Argentina, this genus comprises nine widely distributed and poorly studied species ranging in habitat from tropical to subtropical areas and from sea level to high altitudes.[1a,b] In northeastern Argentina, some species of the Amaryllidaceae family are used in traditional medicine by the Toba indigenous community, including the bulbs of *Hippeastrum parodii* Hunz. & Cocucci for skin disorders (pimples, warts, and skin spots).[2] *Hippeastrum* species have a wide range of biological properties, including cytotoxic,[3] psychoactive,[4] and antifeedant activities.[5] Above all, the Amaryllidaceae family is a well-known source of alkaloids that inhibit acetylcholinesterase (AChE) and, to a lesser extent, butyrylcholinesterase (BuChE) enzymes.[6a−e] Galantamine (Gal), a compound exclusive to Amaryllidaceae, is a long-acting, selective, reversible, and competitive AChE inhibitor, currently used for the treatment of Alzheimer's disease (AD).[7a−c]

As part of an ongoing survey of wild Argentinean Amaryllidaceae species in search of new cholinesterase inhibitors, a phytochemical study of the bulbs of *Hippeastrum argentinum* Pax (Hunz.) collected in central Argentina is described here. Two new (montanine and homolycorine types) and four known alkaloids were isolated and chemically characterized. The cholinesterase (AChE and BuChE)-inhibitory activities of these alkaloids are also reported. For further insight into the experimental results, an in silico study was performed.

## RESULTS AND DISCUSSION

Compounds **1** and **2**, together with the known alkaloids lycorine, montanine, pancracine, and hamayne, were isolated for the first time from the bulbs of *H. argentinum*. The structures of the two new compounds are shown in Figure 1. The alkaloids were identified using GC-MS analysis, which has proven to be a useful tool in the identification of new, known, or unusual structures from alkaloid-rich extracts by comparing their mass fragmentation patterns with standard reference

**Received:** September 1, 2015
**Published:** April 20, 2016





DOI: 10.1021/acs.jnatprod.5b00785
*J. Nat. Prod.* 2016, 79, 1241−1248

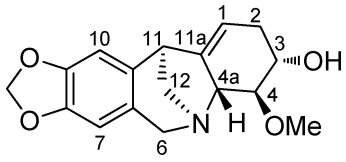


4-*O*-Methylnangustine **1**

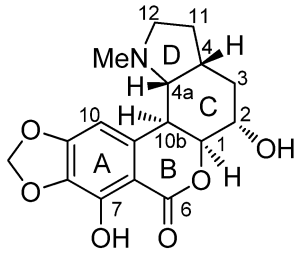


7-Hydroxyclivonine **2**

**Figure 1.**

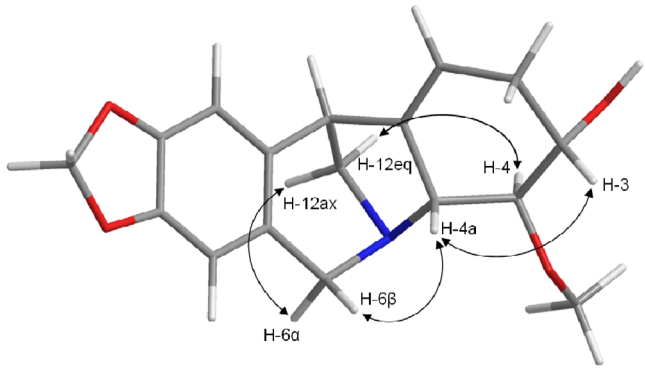


**Figure 2.** Key NOESY correlations of compound **1**. The structures shown here and in Figures 3, 5, and 6 were generated using the PyMOL Molecular Graphics System, version 1.7.4, Schrödinger, LLC.

spectra in homemade databases.[8] This spectrometric technique permitted the detection of 14 compounds, 10 of which were identified as alkaloids from their MS data and retention indexes. The GC-MS profile of the extract is shown in Table 1.

The HRESIMS data for compound **1** suggested a molecular formula of $C_{17}H_{20}NO_4$ for a protonated molecule at *m/z* 302.1388 (calcd 302.1387). The EIMS data for **1** showed a fragmentation pattern similar to that of nangustine, an unusual montanine-type alkaloid isolated from *Narcissus angustifolius* subsp. *transcarpathicus*,[9] with the main difference being that the base peak was 14 units higher, suggesting the presence of an additional methyl or methylene group. This compound was isolated as an amorphous solid and identified as 4-*O*-methylnangustine (Figure 2). The NMR data (500 MHz, $CDCl_3$) summarized in Table 2 were similar to those reported for nangustine,[9] showing two singlets at $\delta$ 6.53 and 6.47 corresponding to H-10 and H-7, respectively. The characteristic methylenedioxy group appeared as two doublets ($\delta$ 5.88, 5.86, *J* = 1.5 Hz), whereas a doublet of triplets at $\delta$ 5.48 was attributed to the olefinic proton (H-1) coupling with the C-2 methylene protons and the H-4a and H-11 allylic protons. The C-6 methylene protons resonated as an AB system at $\delta$ 4.31 and 3.80, showing a geminal coupling constant of 16.6 Hz. A NOESY correlation between H-6$\alpha$ and H-12ax and *W*-coupling between H-6$\beta$ and H-12eq were observed. The main difference relative to nangustine was the presence of a singlet at $\delta$ 3.74 attributed to the methoxy group, which was assigned to C-4 via HMBC data. The C-2 methylene group was established based on the HSQC data and the COSY correlations between H-1 and the C-2 methylene protons, confirming that compound **1** is a C-3/C-4- and not a C-2/C-3-disubstituted alkaloid. The $^{13}C$ NMR spectroscopic data show a singlet at $\delta$ 147.86 attributable to the olefinic C-11a, a characteristic signal of the 5,11-methanomorphanthridine Amaryllidaceae alkaloids.[10] The absolute configuration of this alkaloid was determined by electronic circular dichroism (ECD) spectroscopy, the Cotton effects being similar to those observed for 5,11-methanomorphanthridine alkaloids with an $\alpha$-methylene bridge.[9,10]

Compound **2** was obtained as an amorphous solid. Its molecular formula was confirmed as $C_{17}H_{20}NO_6$ via HRESIMS

**Table 1. GC-MS Analysis of the Alkaloid Content of *Hippeastrum argentinum***

| alkaloid | RI[b] | % in basic $CHCl_3$ extract | $M^+$ | MS |
|---|---|---|---|---|
| Gal | 2402 | 0.343 | 287(83) | 286(100), 270(13), 244(24), 230(12), 216(33), 174(27), 115(12) |
| *m/z* 297 | 2465 | 0.572 | 297(39) | 254(42), 253(36), 224(27), 223(100), 222(13), 181(12), 165(20), 153(21), 152(29) |
| vittatine/crinine[a] | 2499 | 1.171 | 271(100) | 228(25), 199(95), 187(85), 173(28), 128(32), 115(33), 56(22) |
| anhydrolycorine | 2512 | 0.689 | 251(43) | 250(100), 192(13), 191(11), 165(4), 164(3), 139(2), 124(7) |
| 4-*O*-methylnangustine (**1**) | 2529 | 11.821 | 301(100) | 271(34), 254(49), 252(34), 223(29), 212(31), 199(46), 185(77), 141(35), 115(35) |
| 11,12-dehydroanhydrolycorine | 2617 | 1.433 | 249(59) | 248(100), 191(11), 190(27), 189(7), 163(8), 123(7), 95(19), 81(7) |
| montanine | 2651 | 71.954 | 301(100) | 270(87), 257(37), 252(24), 229(26), 226(30), 223(29), 199(20), 185(32), 115(21) |
| pancracine | 2718 | 1.841 | 287(100) | 286(23), 270(19), 243(25), 223(27), 214(24), 199(32), 185(42), 128(21), 115(24) |
| hamayne | 2731 | 2.662 | 287(4) | 259(15), 258(100), 242(10), 211(13), 186(15), 181(17), 128(14), 115(13) |
| lycorine | 2763 | 5.247 | 287(31) | 286(19), 268(24), 250(15), 227(79), 226(100), 211(7), 147(15) |
| *m/z* 287 | 2767 | 0.610 | 287(14) | 286(8), 281(76), 280(100), 268(13), 266(9), 265(9), 250(14), 227(37), 226(63) |
| *m/z* 257 | 2920 | 0.459 | 257(100) | 256(51), 211(7), 188(6), 181(28), 153(9), 152(9), 141(7), 115(11) |
| *m/z* 319 | 2950 | 0.378 | 319(100) | 318(31), 276(21), 274(29), 261(19), 260(26), 243(26), 189(19), 96(21) |
| 7-hydroxyclivonine (**2**) | 3043 | 0.812 | 333(12) | 178(3), 97(5), 96(64), 84(5), 83(100), 82(32), 44(3), 42(8) |

[a]Cannot be distinguished by GC-MS. [b]RI: retention index.



DOI: 10.1021/acs.jnatprod.5b00785
J. Nat. Prod. 2016, 79, 1241−1248

**Table 2. NMR Spectroscopic Data (500 MHz, $CDCl_3$) for 4-*O*-methylnangustine (1)**

| position | $\delta_C$, type | $\delta_H$ ($J$ in Hz) | HMBC[a] |
|---|---|---|---|
| 1 | 113.2, CH | 5.48, dt (3.4, 2.5) | 3, 4a |
| 2$\alpha$ | 33.6, $CH_2$ | 2.11, ddt (17.8, 9.0, 3.4) | 1, 3, 11a |
| 2$\beta$ | | 2.59, dddd (17.7, 7.1, 3.4, 2.1) | 1, 3, 4, 11a |
| 3 | 70.2, CH | 3.73, ddd (9.1, 9.0, 7.1) | 2, 4a |
| 4 | 83.9, CH | 3.03, t (9.2) | 3, 4a, 11a, OMe |
| 4a | 68.4, CH | 3.20, brd (9.2) | 4, 6, 11a |
| 6$\alpha$ | 61.6, $CH_2$ | 4.31, d (16.6) | 4a, 6a, 7, 10a |
| 6$\beta$ | | 3.80, d (16.6) | 4a, 6a, 7, 10a, 12 |
| 6a | 125.1, C | | |
| 7 | 107.0, CH | 6.47, s | 6, 9, 10a |
| 8 | 146.8, C | | |
| 9 | 146.1, C | | |
| 10 | 107.4, CH | 6.53, s | 6a, 8, 11 |
| 10a | 132.7, C | | |
| 11 | 45.1, CH | 3.18, brd (2.5) | 1, 4a, 6a, 10, 10a, 11a |
| 11a | 147.9, C | | |
| 12ax | 56.5, $CH_2$ | 3.02, brd (11.4) | 4a, 6, 10a, 11a |
| 12eq | | 2.96, ddd (11.1, 2.6, 0.6) | 6, 10a, 11a |
| OMe | 59.8, $CH_3$ | 3.74, s | 4 |
| $OCH_2O$ | 100.9, $CH_2$ | 5.88, d–5.86, d (1.5) | 9 |

[a]HMBC correlations, optimized for 8 Hz, are from proton(s) to the indicated carbon.

**Table 3. NMR Spectroscopic Data (500 MHz, Methanol-$d_4$) for 7-Hydroxyclivonine (2)**

| position | $\delta_C$, type | $\delta_H$ ($J$ in Hz) | HMBC[a] |
|---|---|---|---|
| 1 | 83.28, CH | 4.58, dd (6.2, 4.4) | 2, 3, 4a, 6, 10a, 10b, |
| 2 | 68.21, CH | 3.85, ddd (10.8, 6.2, 4.8) | 1, 3, 4, 10b |
| 3$\alpha$ | 33.98, $CH_2$ | 1.58, ddd (13.3, 10.8, 10.6) | 1, 2, 4, 4a, 11 |
| 3$\beta$ | | 1.93, ddd (13.3, 6.1, 4.8) | 1, 2, 4, 4a, 11 |
| 4 | 35.39, CH | 2.33, m (overlapped) | 2, 3, 4a, 11, 12 |
| 4a | 65.91, CH | 2.69, t (7.0) | 1, 3, 4, 10a, 10b, 11, 12, NMe |
| 6 | 168.58, C | | |
| 6a | 103.94, C | | |
| 7 | 146.17, C | | |
| 8 | 154.10, C | | |
| 9 | 133.17, C | | |
| 10 | 99.73, CH | 6.69, d (0.7) | 6, 6a, 7, 8, 9, 10b |
| 10a | 137.73, C | | |
| 10b | 37.57, CH | 3.32, td (7.0, 4.4, 0.7) | 1, 2, 4, 4a, 6a, 10, 10a |
| 11$\alpha$ | 29.76, $CH_2$ | 1.63, dddd (12.4, 8.9, 7.6, 6.6) | 3, 4, 4a, 12 |
| 11$\beta$ | | 2.01, dddd (12.4, 8.0, 7.2, 3.1) | 3, 4, 4a, 12, NMe |
| 12$\alpha$ | 55.25, $CH_2$ | 3.17, ddd (9.5, 7.6, 3.1) | 4, 4a, 11 |
| 12$\beta$ | | 2.32, m (overlapped) | 4, 11, NMe |
| $OCH_2O$ | 102.51, $CH_2$ | 6.06, s | 8, 9 |
| NMe | 41.24, $CH_3$ | 2.16, s | 4a, 12 |

[a]HMBC correlations, optimized for 8 Hz, are from proton(s) to the indicated carbon.

($m/z$ 334.1290 for $[M + H]^+$, calcd 334.1285) and $^{13}C$ NMR data. The mass fragmentation pattern indicated that **2** was related to clivonine, showing typical ions at $m/z$ 82, 83, and 96.[11] The molecular ion at $m/z$ 333, which is 16 units higher than in clivonine, suggests the presence of an additional oxygen functional group. The IR data revealed a band at 1682 $cm^{-1}$, assignable to a carbonyl group conjugated with an aromatic system, which is in agreement with $^{13}C$ NMR data showing a signal at $\delta$ 168.58 (Table 3). The $^1H$ NMR data (500 MHz, methanol-$d_4$) revealed one aromatic proton as a doublet at $\delta$ 6.69 ($J$ = 0.7 Hz). This small benzylic coupling with H-10b, together with the NOESY correlations with both H-10b ($\delta$ 3.32) and the *N*-methyl group ($\delta$ 2.16), permitted its assignment to H-10. The methylenedioxy protons resonated as a broad singlet at $\delta$ 6.06 (2H), whereas a doublet of doublets at $\delta$ 4.58 was assigned to H-1. The lower field position of H-1 suggests an $\alpha$-oriented proton, which is in accordance with the NMR data of other homolycorine-type alkaloids.[12a−c] The $^1H$ NMR spectrum also displayed two doublets of doublets at $\delta$ 3.85 and 3.17, corresponding to H-2 and H-12$\alpha$, respectively, and a triplet at $\delta$ 2.69 attributed to H-4a. NOESY correlations between H-1/H-3$\alpha$, H-4/H-2, and H-4/NMe, together with the *N*-methyl chemical shift ($\delta$ 2.16),[12a] suggest a *cis*-B/C *anti*, *cis*-C/D configuration for compound **2** (Figure 3). The name 7-hydroxyclivonine was proposed for this compound.

The isolated compounds, together with the basic $CHCl_3$ extract, were tested for in vitro AChE- and BuChE-inhibitory activities. The results, expressed as half-maximal inhibitory concentration ($IC_{50}$) values and the selectivity index, calculated as $IC_{50}$AChE/$IC_{50}$BuChE, are summarized in Table 4. Galantamine was used as a positive control. The basic $CHCl_3$ extract showed modest activity against AChE ($IC_{50}$ = 50.2 $\mu$g/mL) and weak activity against BuChE ($IC_{50}$ = 115.5 $\mu$g/mL). Compound **2**, a homolycorine-type alkaloid, exhibited weak AChE inhibition ($IC_{50}$ = 114.07 $\mu$M) but weak to moderate activity against BuChE ($IC_{50}$ = 67.3 $\mu$M), which was 3-fold less than that of Gal ($IC_{50}$ = 22.39 $\mu$M). Interestingly, unlike Gal, compound **2** was moderately selective toward BuChE (SI = 1.69). This is the homolycorine-type alkaloid with the highest inhibition toward BuChE reported to date. Otherwise, as expected, Gal-type alkaloids were the most potent cholinesterase inhibitors among the Amaryllidaceae alkaloids. The other tested compounds did not show inhibitory activity against either enzyme ($IC_{50}$ > 200 $\mu$M).

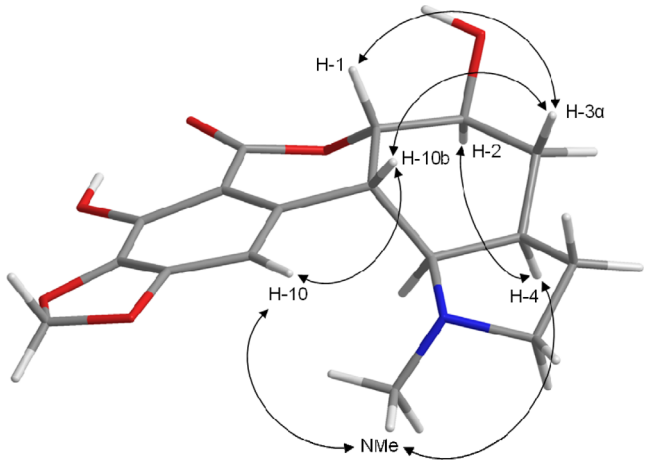


**Figure 3.** Key NOESY correlations of compound **2** (the PyMOL Molecular Graphics System).

**Molecular Modeling.** To better understand the experimental results, a molecular modeling study was conducted to simulate the interactions of compounds **1** and **2** in the catalytic


DOI: 10.1021/acs.jnatprod.5b00785
J. Nat. Prod. 2016, 79, 1241−1248

**Table 4. AChE and BuChE Inhibitory Activities of *Hippeastrum argentinum* Alkaloids**

| compound | $IC_{50}$ ($\mu$M)[a] AChE | BuChE | SI[b] |
|---|---|---|---|
| **1** | >200 | >200 | |
| **2** | 114.07 ± 0.08 | 67.3 ± 0.09 | 1.69 |
| pancracine | >200 | >200 | |
| montanine | >200 | >200 | |
| hamayne | >200 | >200 | |
| lycorine | >200 | >200 | |
| chloroform extract | 50.2 ± 0.12($\mu$g/mL) | 115.5 ± 0.13($\mu$g/mL) | 0.43 |
| Gal[c] | 0.48 ± 0.03 | 22.39 ± 0.09 | 0.02 |

[a]$IC_{50}$ values are expressed as the means ± SD of three replicate determinations. [b]SI is the BuChE selectivity index defined as $IC_{50}$ AChE/$IC_{50}$ BuChE. [c]Reference compound.

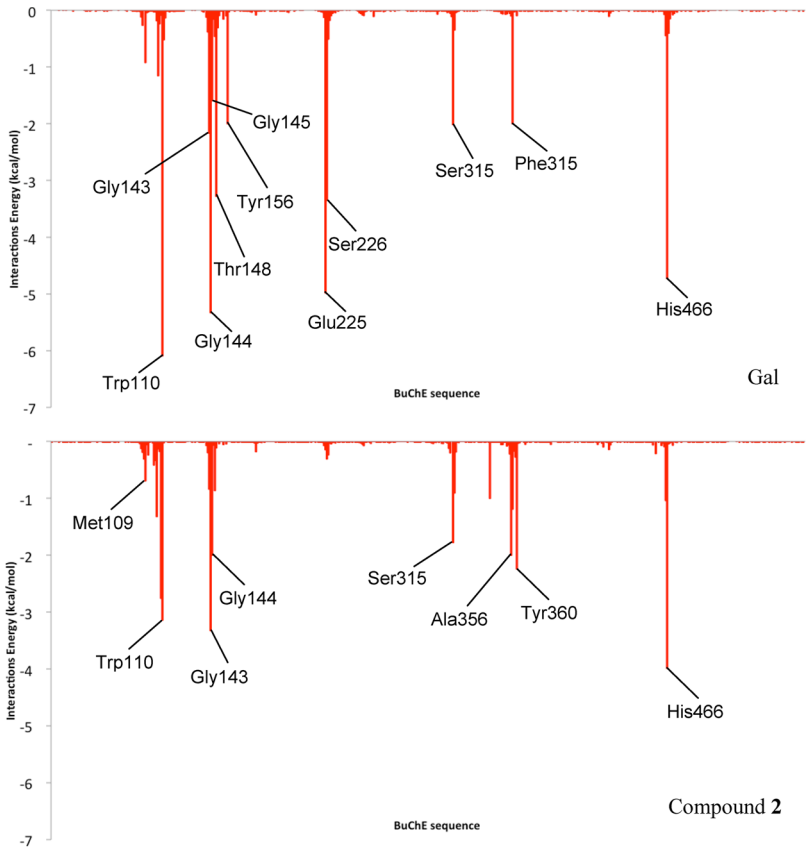


**Figure 4.** Histograms showing the interaction energies of Gal and compound **2** with the main amino acids involved in the complex formation.

site of BuChE. Additionally, molecular simulations of Gal were performed to compare with those of **1** and **2**. The docking study suggested that compounds **1** and **2** would bind in the catalytic site of BuChE similarly to Gal. These results are in agreement with previous reports showing by molecular modeling that different alkaloids interact in the same way as Gal in the active site pocket of AChE.[8,13] Although those studies were conducted with AChE instead of BuChE, several reports have shown that AChE and BuChE share 65% amino acid sequence homology and similar overall structures. Likewise, the catalytic triad Ser−His−Glu, which is essential for cholinesterase activity, is conserved in both AChE and BuChE across species.[8,13−17]

In the second stage of the study, molecular dynamics simulations (MDS) were performed in order to estimate the binding energies of different complexes using molecular mechanics generalized Born solvent accessibility (MM-GBSA) calculations. The MDS predict that the binding energy of Gal is −38.12 kcal/mol, whereas the binding energies for compounds **1** and **2** are −24.96 and −27.82 kcal/mol, respectively. These results are in complete agreement with the experimental data.

To determine which amino acids are involved in the complex formation, the histograms of the interaction energies were studied. The histograms obtained for the complexes of Gal and compound **2** in the catalytic site of BuChE (Figure 4) clearly show that the Gal complex is stabilized by various molecular interactions, mainly, Trp110, Gly144, Glu225, His466, Ser226, Thr148, Gly143, Ser315, Tyr156, Phe357, Gly145, and Ser107.[8,13,18] It should be noted that in the complex of compound **2** several of these interactions have been lost (Glu225, Ser226, Thr148, Gly143, Ser315, Tyr156, Phe357, and Ser107). However, important interactions, such as Trp110,


DOI: 10.1021/acs.jnatprod.5b00785
J. Nat. Prod. 2016, 79, 1241−1248

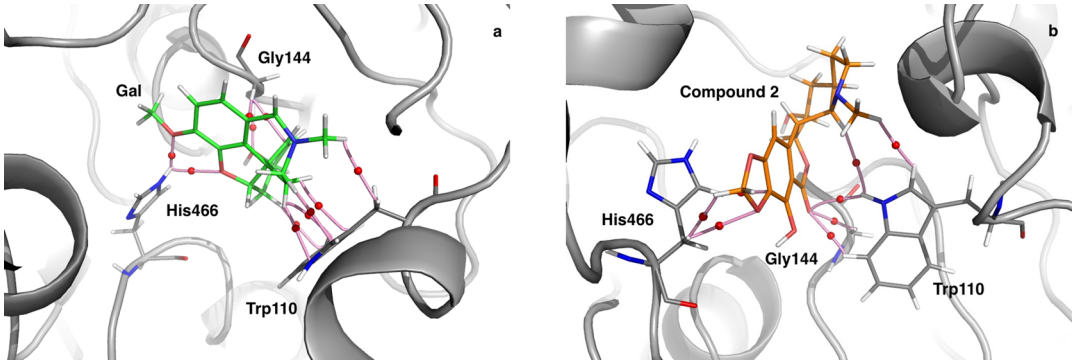


**Figure 5.** Main interactions at the binding pocket of BuChE: (a) Gal (green), (b) compound **2** (orange) (the PyMOL Molecular Graphics System).

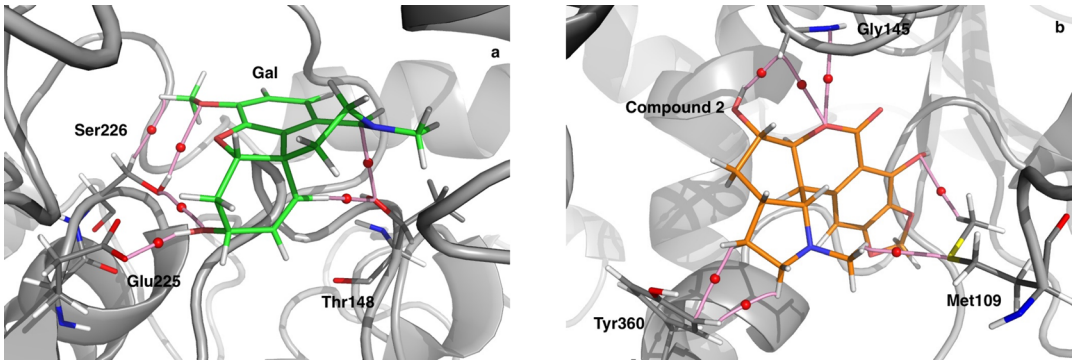


**Figure 6.** Differential interactions displayed by the complexes at the binding pocket of BuChE: (a) Gal (green), (b) compound **2** (orange) (the PyMOL Molecular Graphics System).

Gly144, His466, Ser315, and Gly145, remain, stabilizing the complex with compound **2**. These results explain, at least in part, the inhibitory activity observed for this molecule. In contrast, the stronger interactions observed in the Gal complex might explain why this molecule has a higher inhibitory effect than compound **2**. The results obtained for the complex of compound **1** (Figure S9, Supporting Information) clearly show that it has fewer stabilizing interactions than the previous complexes, which explains its lack of an inhibitory effect on this enzyme.

At this stage, although the trend predicted by the MDS can be considered significant, only weak interactions were investigated. Therefore, reduced models were constructed to perform more accurate DFT calculations [B3LYP/6-1G(d) level], allowing a quantum theory of atoms in molecules (QTAIM) analysis to further characterize the most critical ligand interactions. Figure 5a illustrates the main interactions of Gal at the binding pocket, with Gal establishing three strongly stabilizing interactions with the following amino acids: Trp110, Gly144, and His466. According to the QTAIM analysis, the $\rho_{(rb)}$ values for these interactions are 0.072, 0.045, and 0.037 au, respectively. These three interactions are also present in the complex of compound **2** with BuChE (Figure 5b). The $\rho_{(rb)}$ values obtained for Trp110, Gly144, and His466 in this complex are 0.045, 0.027, and 0.031 au, respectively. It should be noted that the interactions obtained for compound **2** are significantly weaker than those of Gal.

Figure 6 shows the differential interactions displayed by the complexes of Gal and compound **2** with BuChE. Gal displayed stabilizing interactions with Thr148, Glu225, and Ser226, with $\rho_{(rb)}$ values of 0.025, 0.048, and 0.051 au, respectively (Figure 6a). In turn, compound **2** showed interactions with Met109, Gly145, and Tyr360, with $\rho_{(rb)}$ values of 0.015, 0.011, and 0.23 au, respectively (Figure 6b). Once again, these interactions were weaker than those observed for Gal. These results could explain, at least partially, why Gal possesses a stronger inhibitory effect than compound **2**. Figure 7 shows a spatial view of the overlapping of Gal and compound **2** in their respective complexes with BuChE.

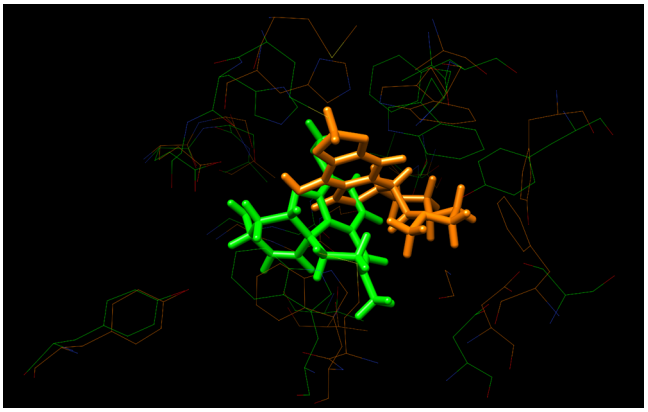

**Figure 7.** Spatial view of the overlapping of Gal (green) and compound **2** (orange) in their respective complexes with BuChE.

Considering that both Gal and compound **2** possess the same pharmacophoric pattern (Figure 8), it is reasonable to assume that the main mechanism of action of this compound could also be the same. However, based on these results, the possibility that compound **2** acts on an allosteric site as a



DOI: 10.1021/acs.jnatprod.5b00785
J. Nat. Prod. 2016, 79, 1241−1248

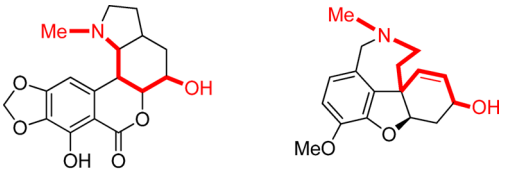


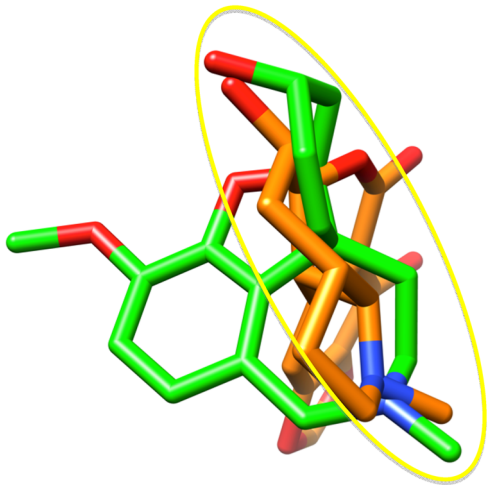

**Figure 8.** Spatial view of Gal (green) and compound **2** (orange) showing the overlapping of their pharmacophoric portions. The groups involved in the pharmacophoric portions of both compounds are schematically denoted in red at the top of this figure.

negative modulator or by some other mechanism cannot be ruled out.

In conclusion, the phytochemical study of *H. argentinum* led to the identification of two new Amaryllidaceae alkaloids and assessment of their cholinesterase-inhibitory activities. The results showed that compound **2** has weak inhibitory activity against BuChE. To better understand the experimental results, a molecular modeling study on the complexes of Gal and compound **2** with BuChE was performed. The results indicate that both compounds interact in the same binding pocket and with similar amino acids. However, the QTAIM analysis suggests that the molecular interactions stabilizing the Gal complex are significantly stronger than those obtained for the complex of compound **2**. These results are in agreement with the experimental data and provide additional support for this study.

## EXPERIMENTAL SECTION

**General Experimental Procedures.** Optical rotations were measured on a PerkinElmer 343 polarimeter (PerkinElmer, Waltham, MA, USA). UV spectra were obtained on a Hewlett-Packard 8453 spectrophotometer (Palo Alto, CA, USA). A Jasco-J-810 spectrophotometer (Easton, MD, USA) was used to record ECD spectra for solutions in MeOH. IR spectra were obtained on an FT-IR Nicolet Magna 550 spectrophotometer (Nicolet Instrumentations, Madison, WI, USA). NMR spectra were recorded on a Mercury 400 MHz (Palo Alto, CA, USA) and a Varian 500 MHz (Palo Alto, CA, USA) instrument using $CDCl_3$ as the solvent for **1** and methanol-$d_4$ as the solvent for **2**. The GC-MS spectra were obtained on an Agilent 6890N GC 5975 inert MSD operating in EI mode at 70 eV (Agilent Technologies, Santa Clara, CA, USA) using a DB5-MS column (30 m × 0.25 mm × 0.25 μm). The temperature program was as follows: 100−180 °C at 15 °C $min^{-1}$, 1 min hold at 180 °C, 180−300 °C at 5 °C $min^{-1}$, and 10 min hold at 300 °C. The injector temperature was 280 °C. The flow rate of the He carrier gas was 0.8 mL $min^{-1}$, and the split ratio was 1:20 (with more diluted samples, a split ratio of 1:5 was applied). A hydrocarbon mixture ($C_9$−$C_{36}$ Restek, cat no. 31614) was used for the retention index calibration. The proportion of each compound in the alkaloid fractions was expressed as a percentage of the total alkaloid content (Table 1). These data do not express quantification, although they can be used to compare the relative abundances of each component. HRESIMS data were obtained via LC/MSD-TOF (Agilent 2006) (Agilent Technologies) by direct injection of the compounds dissolved in MeOH. For analytical and preparative TLC, silica gel $F_{254}$ was used as the stationary phase (20 × 20 cm), whereas column chromatography (CC) was performed using silica gel 60A (6−35 μm). The bands were detected by staining with Dragendorff's reagent. Exclusion chromatography was conducted using Sephadex LH-20. AChE from *Electrophorus electricus* (electric eel) and BuChE from equine serum were obtained from Sigma-Aldrich (St. Louis, MO, USA).

**Plant Material.** Bulbs of *H. argentinum* were collected in Tucumán Province, Argentina, in February 2012 during the flowering period. Plant samples were identified by MSc. German Roitman, Facultad de Agronomía, Capital Federal, Buenos Aires, Argentina. A voucher specimen was deposited at the Instituto de Biotecnología, Universidad Nacional de San Juan, with the code IBT-UNSJ-Arg.15.

**Extraction and Isolation.** Dried bulbs (450 g) were extracted with MeOH (3 × 1000 mL) under reflux for 1 h each. The solvent was evaporated under reduced pressure to obtain 89 g of crude MeOH extract. The extract was dissolved in 2% $H_2SO_4$ (v/v), and neutral material was removed with $Et_2O$ (3 × 200 mL). Then, the aqueous solution was basified with 25% NaOH to pH 10−11 and extracted with $CHCl_3$ (3 × 500 mL) to give the basic $CHCl_3$ extract (3.3 g). Direct precipitation of the extract yielded lycorine (135 mg). The alkaloid extract was roughly separated by $SiO_2$ flash CC using an *n*-hexane/EtOAc/$CH_2Cl_2$/MeOH gradient to give six fractions (A−F): fractions A (*n*-hexane/EtOAc, 1:4), B (EtOAc), C (EtOAc/$CH_2Cl_2$, 1:1), D (EtOAc/MeOH, 9.5:0.5), E (EtOAc/MeOH, 9:1), and F (MeOH). Montanine (800 mg) precipitated spontaneously from fraction D. Column chromatography on Sephadex LH-20 of fraction A in MeOH gave three subfractions. Fraction A1 was consecutively chromatographed on a silica gel column (CC) using gradient elution from *n*-hexane/EtOAc (2:8−0:10) to EtOAc/MeOH (9:1) to give six subfractions (A1a−A1f). Column fractions were monitored by TLC, and similar ones were combined and evaporated to dryness. Crystallization of fraction A1c afforded 7-hydroxyclivonine (**2**) (12 mg). Column chromatography on Sephadex LH-20 of fraction B in MeOH gave three subfractions. Subfraction B1 was subjected to preparative TLC (silica gel with *n*-hexane/EtOAc/$CHCl_3$/MeOH, 3:4:2:1, in $NH_3$ atmosphere) to give 4-*O*-methylnangustine (**1**) (15 mg). Subfraction B2 was subjected to CC on silica gel eluted with $CHCl_3$/MeOH (95:5) to afford pancracine (20 mg) and hamayne (10 mg).

*4-O-Methylnangustine (**1**):* yellow, amorphous solid; $[\alpha]^{25}_D$ −17.7 (*c* 0.3, $CHCl_3$); UV ($CHCl_3$) $\lambda_{max}$ (log ε) 245 (1.01), 296 (0.99) nm; ECD (*c* 3.32 × $10^{-3}$ M, MeOH) $[\theta]_{257}$ −19879, $[\theta]_{269}$ −2710, $[\theta]_{307}$ −2409; IR (film) $\nu_{max}$ 2925, 2360, 2342, 1732, 1505, 1484, 1373, 1332, 1235, 1200, 1139, 1099, 1038, 994, 935, 892, 860, 822, 759, 668, 617, 545, 428, 404 $cm^{-1}$; $^1H$ NMR ($CDCl_3$, 500 MHz) and $^{13}C$ NMR ($CDCl_3$, 125 MHz), see Table 2; HRESIMS *m*/*z* 302.1388 $[M + H]^+$ (calcd for $C_{17}H_{20}NO_4$, 302.1387); EIMS data shown in Table 1.

*7-Hydroxyclivonine (**2**):* colorless, amorphous solid; $[\alpha]^{25}_D$ −4.8 (*c* 0.2, MeOH); UV (MeOH) $\lambda_{max}$ (log ε) 213 (1.82), 237 (1.88), 286 (1.45) nm; IR (film) $\nu_{max}$ 2925, 2357, 1683, 1636, 1507, 1489, 1457, 1274, 1079, 1029, 468 $cm^{-1}$; $^1H$ NMR (methanol-$d_4$, 500 MHz) and $^{13}C$ NMR (methanol-$d_4$, 125 MHz), see Table 3; HRESIMS *m*/*z* 334.1290 $[M + H]^+$ (calcd for $C_{17}H_{20}NO_6$, 334.1285); EIMS data shown in Table 1.

Lycorine,[19a,b] montanine,[20] pancracine,[9,10] and hamayne[21] were identified by direct comparison of their chromatographic and spectroscopic properties with those of authentic samples obtained in our laboratory from other plant sources and the reported data.



DOI: 10.1021/acs.jnatprod.5b00785
J. Nat. Prod. 2016, 79, 1241−1248

**Microplate Assay for AChE- and BuChE-Inhibitory Activities.** Cholinesterase inhibitory activities were performed according to Ellman et al.[22] with some modifications.[6a] Fifty microliters of AChE or BuChE in phosphate buffer (8 mM $K_2HPO_4$, 2.3 mM $NaH_2PO_4$, 0.15 M NaCl, pH 7.6) and 50 $\mu$L of the sample dissolved in the same buffer were added to the wells. The plates were incubated for 30 min at room temperature before 100 $\mu$L of the substrate solution (0.1 M $Na_2HPO_4$, 0.5 M DTNB, and 0.6 mM ATCI in Millipore water, pH 7.5) was added. The absorbance was read in a Thermo Scientific Multiskan FC microplate spectrophotometer at 405 nm after 5 min. The enzyme-inhibitory activity was calculated as a percentage compared to an assay using a buffer without any inhibitor. The enzyme-inhibitory data were analyzed with the software package Prism (Graph Pad Inc., San Diego, CA, USA). The compound **2** concentrations used to calculate the $IC_{50}$ values were 15, 30, 60, 120, 160, and 200 $\mu$M in both AChE and BuChE assays. The $IC_{50}$ values are the means ± SD of three individual determinations, each performed in triplicate.

**Automated Docking Setup.** X-ray structures available in the Protein Data Bank (http://www.rcsb.org) were used as follows: *Ee*AChE (1C2O)[23] and eqBuChE (UniProtAC Q9N1N9).[24a−d] Molecular docking was conducted using AutoDock Vina.[25] This program was adopted to perform molecular docking; the receptor structure was defined as rigid, and the grid dimensions were 25, 25, and 25 for the X, Y, and Z axes, respectively, in the catalytic site region with a resolution of 0.375 Å. Gasteiger charges were assigned for all the compounds, and nonpolar hydrogen atoms were merged. All torsions of the ligand were allowed to rotate during docking. The value for the exhaustiveness of the search was 400, whereas the number of poses collected was 10. All graphic manipulations and visualizations were performed using the AutoDock Tools 1.5.4[26] and ligand docking with Autodock Vina 1.1.1.[25]

**MDS.** The complex geometries from docking were soaked in boxes of explicit water using the TIP3P model[27] and subjected to MDS. All MDS were performed with the Amber software package using periodic boundary conditions and cubic simulation cells. The particle mesh Ewald method[28] was applied using a grid spacing of 1.2 Å, a spline interpolation order of 4, and a real space direct sum cutoff of 10 Å. The SHAKE algorithm was applied allowing for an integration time step of 2 fs. MDS were carried out at a 300 K target temperature and extended to 5 ns overall simulation time. The isothermal−isobaric (NPT) ensemble was employed using Berendsen coupling to a baro/thermostat (target pressure 1 atm, relaxation time 0.1 ps). Post MD analysis was performed with the program PTRAJ.[29]

**MM-GBSA Free Energy Decomposition.** To determine the residues of the BuChE catalytic site involved in the interactions, histograms of the interaction energy were used. The MM-GBSA free energy decomposition using the mm_pbsa program in AMBER12 was employed to corroborate the amino acids interacting with the ligands. This calculation can decompose the interaction energies of each residue, considering the molecular mechanics and solvation energies.[30a,b] Each ligand−residue pair includes four energy terms: van der Waals contribution ($E_{vdw}$), electrostatic contribution ($E_{ele}$), a polar desolvation term ($G_{GB}$), and a nonpolar desolvation term ($G_{SA}$); they are summarized in the following equation: $\Delta G_{\text{inhibitor residue}} = \Delta E_{vdw} + \Delta E_{ele} + \Delta G_{GB} + \Delta G_{SA}$. For MM-GBSA methodology, snapshots were taken at 10 ps time intervals from the corresponding last 1000 ps MD trajectories, and the explicit water molecules were removed from the snapshots.

**QTAIM.** After the QM/MM calculation, the optimized geometries were used as input for QTAIM analysis,[31] which was performed with the help of Multiwfn software[32] using the wave functions generated at the B3LYP-D/6-31G(d) level. This type of calculation has been used in recent studies because it ensures a reasonable compromise between the wave function quality required to obtain reliable values of $\rho(r)$ and the available computer power, considering the extension of the system in the study.[33a−d]

## ■ ASSOCIATED CONTENT

### Supporting Information

The Supporting Information is available free of charge on the ACS Publications website at DOI: 10.1021/acs.jnatprod.5b00785.

$^1$H, $^{13}$C, COSY, and NOESY spectra and the histogram of interaction energies obtained for the complexes of compound **1** with BuChE (PDF)

## ■ AUTHOR INFORMATION


### Corresponding Author

*E-mail (G. Feresin): gferesin@unsj.edu.ar. Tel: +54 264 4211700, int. 410. Fax: +54 264 4213672.


### Notes

The authors declare no competing financial interest.

## ■ ACKNOWLEDGMENTS


The authors wish to thank ANPCyT (PICTO2009-0116), PICT 2014-3425, and CICITCA-UNSJ (80020130100449SJ) for financial support. J.B. (Research Group 2014-SGR-920) is grateful to the SCT-UB for technical support. J.O. holds a fellowship from CONICET. G.E.F., N.P., S.A.A., and R.D.E. are researchers from CONICET. The authors would like to thank MSc. D. Zamo for technical assistance.


## ■ REFERENCES


(1) (a) Zuloaga, F. O.; Morrone, O.; Belgrano, M. J. In *Catálogo de las plantas vasculares del Cono Sur (Argentina, sur de Brasil, Chile, Paraguay, y Uruguay) Ptherydophyta, Gymnospernae, Monocotyledoneae*, Monographs in Systematic Botany from the Missouri Botanical Garden; 2008; Vol. *1*, pp 1−983. (b) Sultana, J.; Sultana, N.; Siddique, M. N. A.; Islam, A. K. M. A.; Hossain, M. M.; Hossain, T. *J. Cent. Eur. Agric.* **2010**, *11*, 469−474.

(2) Martínez, G. J.; Barboza, G. E. *J. Ethnopharmacol.* **2010**, *132*, 86−100.

(3) Silva, A. F. S.; de Andrade, J. P.; Machado, K. R. B.; Rocha, A. B.; Apel, M. A.; Sobral, M. E. G.; Henriques, A. T.; Zuanazzi, J. A. S. *Phytomedicine* **2008**, *15*, 882−885.

(4) Schürmann da Silva, A. F.; de Andrade, J. P.; Bevilaqua, L. R. M.; de Souza, M. M.; Izquierdo, I.; Henriques, A. T.; Zuanazzi, J. A. S. *Pharmacol., Biochem. Behav.* **2006**, *85*, 148−154.

(5) Santana, O.; Reina, M.; Anaya, A. L.; Hernandez, F.; Izquierdo, M. E.; Gonzalez-Coloma, A. *Z. Naturforsch., C: J. Biosci.* **2008**, *63* (9−10), 639−643.

(6) (a) López, S.; Bastida, J.; Viladomat, F.; Codina, C. *Life Sci.* **2002**, *71*, 2521−2529. (b) Elgorashi, E. E.; Stafford, G. I.; Van Staden, J. *Planta Med.* **2004**, *70* (3), 260−262. (c) Berkov, S.; Codina, C.; Viladomat, F.; Bastida, J. *Bioorg. Med. Chem. Lett.* **2008**, *18* (7), 2263−2266. (d) Konrath, E. L.; Passos dos Santos, C.; Klein, L. C., Jr.; Henriques, A. T. *J. Pharm. Pharmacol.* **2013**, *65* (12), 1701−1725. (e) Pinho, B. R.; Ferreres, F.; Valentão, P.; Andrade, P. B. *J. Pharm. Pharmacol.* **2013**, *65* (12), 1681−1700.

(7) (a) Berkov, S.; Viladomat, F.; Codina, C.; Suárez, S.; Ravelo, A.; Bastida, J. *J. Mass Spectrom.* **2012**, *47* (8), 1065−1073. (b) Yiannopoulou, K. G.; Papageorgiou, S. G. *Ther. Adv. Neurol. Disord.* **2013**, *6* (1), 19−33. (c) Tokuchi, R.; Hishikawa, N.; Matsuzono, K.; Takao, Y.; Wakutani, Y.; Sato, K.; Kono, S.; Ohta, Y.; Deguchi, K.; Yamashita, T.; Abe, K. *Geriatr. Gerontol. Int.* **2016**, *16* (4), 440−445.

(8) Cortes, N.; Alvarez, R.; Osorio, E. H.; Alzate, F.; Berkov, S.; Osorio, E. *J. Pharm. Biomed. Anal.* **2015**, *102*, 222−228.

(9) Labraña, J.; Machocho, A. K.; Kricsfalusy, V.; Brun, R.; Codina, C.; Viladomat, F.; Bastida, J. *Phytochemistry* **2002**, *60*, 847−852.

(10) Ali, A. A.; Mesbah, M. K.; Frahm, A. W. *Planta Med.* **1984**, *50*, 188−189.




DOI: 10.1021/acs.jnatprod.5b00785
*J. Nat. Prod.* 2016, 79, 1241−1248

(11) Ali, A. A.; Ross, S. A.; El-Moghazy, A. M.; El-Moghazy, S. A. *J. Nat. Prod.* **1983**, *46*, 350−352.
(12) (a) Jeffs, P. W.; Mueller, L.; Abou-Donia, A. H.; Seif El-Din, A. A.; Campau, D. *J. Nat. Prod.* **1988**, *51*, 549−554. (b) Pigni, N. B.; Ríos-Ruiz, S.; Martínez-Francés, V.; Nair, J. J.; Viladomat, F.; Codina, C.; Bastida, J. *J. Nat. Prod.* **2012**, *75*, 1643−1647. (c) Giordani, R. B.; de Andrade, J. P.; Verli, H.; Dutilh, J. H.; Henriques, A. T.; Berkov, S.; Bastida, J.; Zuanazzi, J. A. S. *Magn. Reson. Chem.* **2011**, *49*, 668−672.
(13) Lee, S. S.; Venkatesham, U.; Rao, C. P.; Lam, S. H.; Lin, J. H. *Bioorg. Med. Chem.* **2007**, *15*, 1034−1043.
(14) Cheung, J.; Rudolph, M. J.; Burshteyn, F.; Cassidy, M. S.; Gary, E. N.; Love, J.; Franklin, M. C.; Height, J. J. *J. Med. Chem.* **2012**, *55*, 10282−10286.
(15) Brus, B.; Košak, U.; Turk, S.; Pišlar, A.; Coquelle, N.; Kos, J.; Stojan, J.; Colletier, J. P.; Gobec, S. *J. Med. Chem.* **2014**, *57*, 8167−8179.
(16) Khan, M. T. H. *New Biotechnol.* **2009**, *25* (5), 331−346.
(17) Atanasova, M.; Stavrakov, G.; Philipova, I.; Zheleva, D.; Yordanov, N.; Doytchinova, I. *Bioorg. Med. Chem.* **2015**, *23* (17), 5382−5389.
(18) Morris, G. M.; Green, L. G.; Radić, Z.; Taylor, P.; Sharpless, K. B.; Olson, A. J.; Grynszpan, F. *J. Chem. Inf. Model.* **2013**, *53*, 898−906.
(19) (a) Likhitwitayawuid, K.; Angerhofer, C. K.; Chai, H.; Pezzuto, J. M.; Cordell, G. A.; Ruangrungsi, N. *J. Nat. Prod.* **1993**, *56*, 1331−1338. (b) Bastida, J.; Fernández, J.; Viladomat, F.; Codina, C.; Fuente, G. *Phytochemistry* **1995**, *38*, 549−551.
(20) Ishizaki, M.; Hoshino, O.; Iitaka, Y. *J. Org. Chem.* **1992**, *57*, 7285−7295.
(21) Viladomat, F.; Bastida, J.; Codina, C.; Campbell, W. E.; Mathee, S. *Phytochemistry* **1994**, *35*, 809−812.
(22) Ellman, G. L.; Courtney, K. D.; Andres, V.; Featherstone, R. M. *Biochem. Pharmacol.* **1961**, *7*, 88−95.
(23) Bourne, Y.; Grassi, J.; Bougis, P. E.; Marchot, P. *J. Biol. Chem.* **1999**, *274*, 30370−30376.
(24) (a) de Aquino, R. A. N.; Modolo, L. V.; Alvesa, R. B.; de Fátima, A. *Org. Biomol. Chem.* **2013**, *11*, 8395−8409. (b) Arnold, K.; Bordoli, L.; Kopp, J.; Schwede, T. *Bioinformatics* **2006**, *22*, 195−201. (c) Schwede, T.; Kopp, J.; Guex, N.; Peitsch, M. C. *Nucleic Acids Res.* **2003**, *31*, 3381−3385. (d) Guex, N.; Peitsch, M. C. *Electrophoresis* **1997**, *18*, 2714−2723.
(25) Trott, O.; Olson, A. J. *J. Comput. Chem.* **2010**, *31*, 455−461.
(26) Sanner, M. F. *J. Mol. Graph. Model.* **1999**, *17*, 57−61.
(27) Jorgensen, W. L.; Chandrasekhar, J.; Madura, J. D.; Impey, R. W.; Klein, M. L. *J. Chem. Phys.* **1983**, *79*, 926−935.
(28) Darden, T.; York, D.; Pedersen, L. *J. Chem. Phys.* **1993**, *98*, 10089−10092.
(29) Case, D. A.; Cheatham, T. E.; Darden, T.; Gohlke, H.; Luo, R.; Merz, K. M., Jr.; Onufriev, A.; Simmerling, C.; Wang, B.; Woods, R. J. *J. Comput. Chem.* **2005**, *26*, 1668−1688.
(30) (a) Hou, T.; Li, N.; Li, Y.; Wang, W. *J. Proteome Res.* **2012**, *11*, 2982−2995. (b) Gohlke, H.; Kiel, C.; Case, D. A. *J. Mol. Biol.* **2003**, *330*, 891−913.
(31) Bader, R. F. W. *Acc. Chem. Res.* **1985**, *18*, 9−15.
(32) Lu, T.; Chen, F. J. *J. Comput. Chem.* **2012**, *33*, 580−592.
(33) (a) Tosso, R. D.; Andujar, S. A.; Gutierrez, L.; Angelina, E.; Rodríguez, R.; Nogueras, M.; Baldoni, H.; Suvire, F. D.; Cobo, J.; Enriz, R. D. *J. Chem. Inf. Model.* **2013**, *53*, 2018−2032. (b) Andujar, S. A.; Tosso, R. D.; Suvire, F. D.; Angelina, E.; Peruchena, N.; Cabedo, N.; Cortes, D.; Enriz, R. D. *J. Chem. Inf. Model.* **2012**, *52*, 99−112. (c) Gutierrez, L. J.; Barrera Guisasola, E. E.; Peruchena, N.; Enriz, R. D. *Mol. Simul.* **2016**, *42* (3), 196−207. (d) Vega-Hissi, E. G.; Tosso, R.; Enriz, R. D.; Gutierrez, L. J. *Int. J. Quantum Chem.* **2015**, *115*, 389−397.



DOI: 10.1021/acs.jnatprod.5b00785
*J. Nat. Prod.* 2016, 79, 1241−1248